https://doi.org/10.46344/JBINO.2022.v11i04.14

ANALYSIS OF QUANTUM-CHEMICAL INTERACTIONS BETWEEN MALIC ACID AND BRANCHED CHAIN AMINO ACIDS

[1,2] Manuel González-Pérez, [1]Carolina Biviano-Pérez, [1]Víctor Hugo Caro-Gasca, [1]Antonino Benito Piña-Natoli, [1]Gilberto Dorantes-Bautista, [2]Vázquez-González Cecilia, [2]Castro-Díaz Alfredo Salvador.

[1]Tecnológico Nacional de México, Campus Tepeaca (TecNM Campus Tepeaca). Ingeniería en Industrias Alimentarias.

[2]Universidad Tecnológica de Tecamachalco (UTTCAM). Ingeniería en Agricultura Sustentable y Protegida. Ingeniería en Procesos Bioalimentarios.

E-mail: manuel.gp@tepeaca.tecnm.mx

ABSTRACT

Dragon fruit contains 0.2 - 0.35 mg of malic acid (MAC) per 100 g fresh weight. The catabolism of branched-chain amino acids (BCAAs) in osteosarcoma (OS) progression samples and cell lines demonstrates that the ANGPTL4/BCAA/mTOR axis is an essential pathway in OS progression. This research aimed to study the quantum-chemical interaction of malic acid (MAC)and the amino acids (AAs) of cell proteins. This study emphasized the branched chain AAs: valine, leucine, and isoleucine. The hamiltonian combinatorial theory was used to perform all the valence electron jumps between each substance, atom by an atom of each molecule. We used the parameterized semi-empirical model Hyper Chem number 3 (SE-PM3), and the geometry was optimized with the Polak Ribiere method. As a result, interactions of BCVAAs and MAC are very likely and akin. In these three interactions, the oxidative character of MAC is shown. The oxidative character has values very close to each other. This proximity of values indicates a very similar affinity between the MAC and each of the BCVAA. The quantum chemical oxidation of AAs is an antioxidant for another type of interaction since MAC already oxidizes the BCVAA molecule.

Keywords: Malic acid, Dragon fruit, BCAA, ANGPTL4, mTOR, Quantum Chemistry, Hyperchem.

1. INTRODUCTION

1.1 AAs and cancer cells.

AAs help cancer cells (CC) to counteract therapies. This help is due to maintaining CC redox homeostasis, biosynthetic processes, epigenetic modification, and metabolic intermediates for energy generation. Yoo and Hand (2022); Ma et al. (2022); Khan (2022). [1,2,3]

In investigations of the negative relationship between Angiopoietin-like 4 (ANGPTL4) expression and branched-chain AA (BCAA) catabolism in osteosarcoma (OS) progression samples and cell lines. It was concluded that the deletion of ANGPTL4 in cells of the metabolic system resulted in the accumulation of BCAAs, which activated the mTOR protein signaling pathway. This removal enhanced the proliferation of the cells in the system. Taken together, reduced ANGPTL4 expression is associated with OS progression and demonstrates that the ANGPTL4/BCAA/mTOR axis is an essential pathway in OS progression and may be a potential therapeutic target to delay OS progression. The SO. Lin et al. (2022). [4]

1.2 Malic acid.

Das et al. (2022)5 investigated eight blueberry cultivars at three developmental stages to determine the metabolite profile, antioxidant, and anticancer activities and to determine cultivar variations and developmental stages in total phenolic antioxidants, flavonoids, DPPH, and antioxidant assays. FRAP. Multivariate statistical analysis identified five metabolites: quinic acid, methyl succinic acid, chlorogenic acid, oxoadipic acid, and malic acid. All correlations were very high and positive with all anticancer activities.

Ersoy et al. (2022) 6 investigated the extract of the Cerinthe minor plant. They found that 11 different components were present in the extract. The main compounds were malic acid (5392.18±60.93 µg/g extract), fumaric acid (4730.99±58.66 µg/g extract), and rosmarinic acid (2470.07±176.12 µg/g extract). The extract had moderate antioxidant activity, while no inhibitory activity was exerted against the tested enzymes. No cytotoxic activity was observed in human renal (A498, UO-31) or human colon (COLO205, KM12) cancer cell lines.

Potapenko et al. (2022)7 determined that in the presence of L-cysteine, the fluorescence signal of L-malic acid-capped CdS quantum dots is drastically quenched. This study determines the excellent potential of nanocrystals as biosensors of L-cysteine.

In general, the ANGPTL4/BCAA/mTOR triad system is responsible for resisting therapies against cancer cell proliferation. On the other hand, it is observed in several studies that malic acid, accompanied by other metabolites, has antioxidant and anticancer power.
Our goal was to study the quantum-chemical interaction of malic acid and AAs in cells. In this study, we emphasized the branched-chain AAs: valine, leucine, and isoleucine.

2. MATERIAL AND METHODS

2.1 Hamiltonian technique.

The hamiltonian combinatorial theory was used to perform all the valence electron jumps between each substance, atom by an atom of each molecule.

2.2 Quantum methodology:
The molecular simulator Hyper Chem (HC) was purchased. (Hyper Chem. Hypercube, MultiON for Windows. Serial #12-800-1501800080. MultiON. Insurgentes Sur 1236 - 301 Tlacoquemecatl Col. del Valle,

Delegación Benito Juárez, D. F., México CP. 03200).

We use the Hyper Chem parameterized semi-empirical model number 3 (SE-PM3) to draw the corresponding molecules. We then selected SE-PM3. He optimized the geometry with the Polak Ribiere method. He calculated the variables of HOMO-LUMO, BG, EP, and other properties. The results are displayed in column-delimited tables for each concept used in the calculations.
The specific parameters selected for each simulation were the following: SET UP. Semi-empirical method: PM3. Semiempirical Options: Load and Spin. Total Load 0. Multiplicity Turn 1. SCF Control. Convergent limit 0.01. Interaction Limit 1000. Speed Up Converge Yes. Lowest matchmaking spin. Superimposition of weighting factors Sigma-Sigma 1, Pi-Pi1. Polarizabilities were not calculated.

CALCULATION 1. Geometry optimization. Polak Ribiere algorithm (conjugate gradient). Options Termination conditions. RMS gradient of 0.1 kcal/mol or 1000 cycles maximum. Empty, yes. Screen update period one cycle.

CALCULUS 2. Orbitals. Plot orbital options Isosurface representation. Orbital contour value 0.05. Wire mesh isosurface grid. Grid meshes size Coarse. Default grid layout. Default beam contour. Transparency level Default.

CALCULATE 3. Molecular drawings and calculations. Plot molecular options. Molecular Properties. Properties. Electrostatic potential Yes. Representations. Isosurface mapped in 3D. Grid meshes size Coarse. Default grid layout. Irregular Curve Default. Rereading of Isosurfaces. Total Charge Density Contour Value (TCDCV) 0.015. Wire mesh. Transparency level Default. Assigned options Default functions. [8-12]

2.3 The symbols for the interpretation of results are presented below.

Two diagrams are shown in Figure 1. Diagram A presents us with the locus of the quantum well of interactions. The y-axis represents the equivalent number of times the Bohr radius. This number of times is only to compare the jump of the electron from one molecule to another. Diagram B represents the bottoms of the wells in parametric form. The dotted lines are the boundaries between the ETCs of the pure substances. The points show us the value of the oxidation-reduction reactions of the same substances interacting. Three probability areas are displayed: high (bottom), medium (middle), and low (top). The scale of these areas on the left is the same as the quantum well.

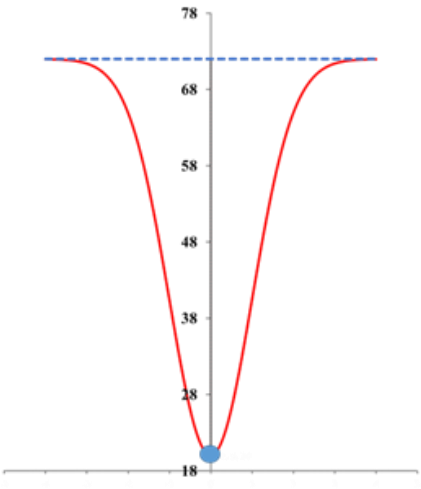

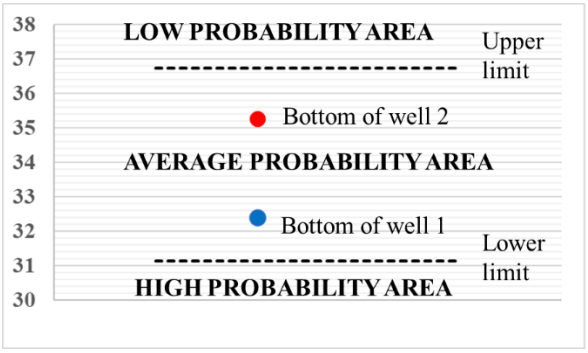

A) Quantum well. Axis "y" radii of Bohr.

B) Diagrams of bottoms of quantum wells and areas of the probabilities of molecular interactions.

Figure 1. Diagrams to interpret quantum interactions between molecules. In Figure B the dotted lines are the bottoms of the wells for pure substances, and the colored dots are the bottoms of the wells for oxidation-reduction interactions. The loci of each well are omitted for space reasons.

3. RESULTS

3.1 Pure substances.

Table 1 shows us the result of all the quantum calculations. Column 1 refers to the sequential order from bottom to top (quantum well). Columns 2 to 9 show the results of all the concepts involved in the calculation. Column 10 displays the value of the ETCs. The value of each ETC can be interpreted as the time number of times the electron jump from the HOMO-LUMO of the same molecule substance. This value is equivalent to the Bohr radius. In the last column, the equivalence is made in nanometers only to know the difference between each substance.

Malic acid (interaction 17) has an estimated 1.959-nanometer jump of the electron from molecule to molecule. This calculation in nanometers gives us an idea that malic acid is not very stable concerning all AAs below that value.

It is emphasized that the most stable AA is Arg (interaction 1, ETC = 26.742, equivalent = 1.415 nm) and the least stable AA is Val (Interaction 21 ETC = 45,188, equivalent = 2.391 nm).

Table 1. AAs and malic acid, ordered. QUANTUM WELL.

No.	Reducing agent	Oxidizing agent	HOMO	LUMO	Bg	δ–	δ+	EP	ETC	Length (nm)
21	Val	Val	-9.914	0.931	10.845	-0.131	0.109	0.240	45.188	2.391
20	Ala	Ala	-9.879	0.749	10.628	-0.124	0.132	0.256	41.515	2.197
19	Leu	Leu	-9.645	0.922	10.567	-0.126	0.130	0.256	41.279	2.184
18	Phe	Phe	-9.553	0.283	9.836	-0.126	0.127	0.253	38.879	2.057
17	MAC	MAC	-11.410	0.548	11.958	-0.125	0.198	0.323	37.022	1.959
16	Gly	Gly	-9.902	0.902	10.804	-0.137	0.159	0.296	36.500	1.931
15	Ser	Ser	-10.156	0.565	10.721	-0.108	0.198	0.306	35.037	1.854
14	Cys	Cys	-9.639	-0.236	9.403	-0.129	0.140	0.269	34.956	1.850
13	Glu	Glu	-10.374	0.438	10.812	-0.111	0.201	0.312	34.655	1.834
12	Ile	Ile	-9.872	0.972	10.844	-0.128	0.188	0.316	34.316	1.816
11	Thr	Thr	-9.896	0.832	10.728	-0.123	0.191	0.314	34.167	1.808
10	Gln	Gln	-10.023	0.755	10.778	-0.124	0.192	0.316	34.108	1.805
9	Asp	Asp	-10.370	0.420	10.790	-0.118	0.204	0.322	33.509	1.773
8	Asn	Asn	-9.929	0.644	10.573	-0.125	0.193	0.318	33.249	1.759
7	Lys	Lys	-9.521	0.943	10.463	-0.127	0.195	0.322	32.495	1.719
6	Pro	Pro	-9.447	0.792	10.238	-0.128	0.191	0.319	32.095	1.698
5	Trp	Trp	-8.299	0.133	8.431	-0.112	0.155	0.267	31.577	1.671
4	Tyr	Tyr	-9.056	0.293	9.349	-0.123	0.193	0.316	29.584	1.565
3	His	His	-9.307	0.503	9.811	-0.169	0.171	0.340	28.855	1.527
2	Met	Met	-9.062	0.145	9.207	-0.134	0.192	0.326	28.243	1.494
1	Arg	Arg	-9.176	0.558	9.734	-0.165	0.199	0.364	26.742	1.415

3.2 MAC vs. BCAA.

Table 2 shows the specific interaction between MAC and the branched AA valine. The first two lines show the two pure

substances that interact. In row 3, we can see the MAC-Val interaction with an ETC = 52.741 Bohr radii. In this interaction, valine oxidizes MAC.

Row 4 shows the Val-MAC interaction with an ETC = 31.798 Bohr radii. In this interaction, the MAC oxidizes the AA valine.

Table 2. Specific interaction between MAC and the AA valine.

Nombre	Reducing agent	Oxidizing agent	HOMO	LUMO	Bg	δ–	δ+	EP	ETC
Ac. Málico	MAC	MAC	-11.410	0.548	11.958	-0.125	0.198	0.323	37.022
Valina	Val	Val	-9.914	0.931	10.845	-0.131	0.109	0.24	45.188
Ac. Málico vs. Valina	MAC	Val	-11.410	0.931	12.341	-0.125	0.109	0.234	52.741
Valina vs. Ac. Málico	Val	MAC	-9.914	0.548	10.462	-0.131	0.198	0.329	31.798

The bottoms of the quantum wells are shown in Figure 2 (see Figure 1B). The red dot representing the Val-MAC interaction falls in the high-probability zone. For this reason, MAC will oxidize the AA Val with a high probability. Instead, the blue dot falls in the zone of lowest probability; the AA Val has a very low probability of oxidizing MAC.

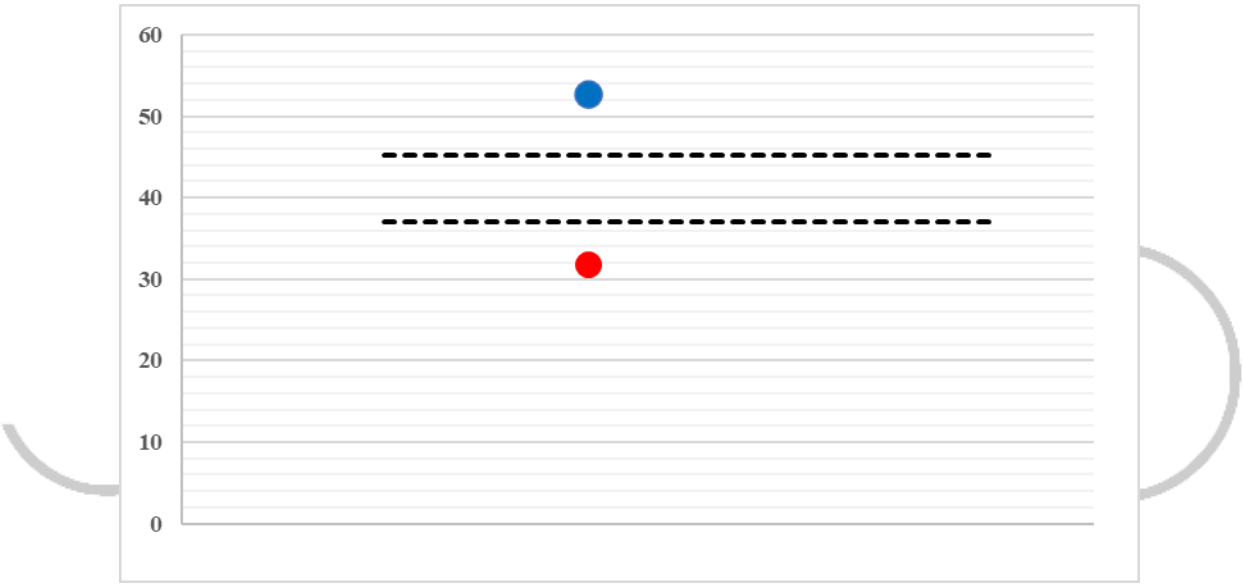

Figure 2. Diagram of four quantum well bottoms compared parametrically. Dotted lines, pure substances. Points, oxidation-reduction interactions. The red dot (Val-MAC) is in a zone of high probability or affinity, and the blue (MAC-Val) is in a low probability zone. In all interactions Left = reducing agent, Right = oxidizing agent.

Table 3 shows the specific interaction between MAC and the branched AA leucine. The first two lines show the two pure substances that interact. In row 3, we can see the MAC-Leu interaction with an ETC = 48.362 Bohr radii. In this interaction, leucine oxidizes MAC.

Row 4 shows the Leu-MAC interaction with ETC = 31.460 Bohr radii. In this interaction, the MAC oxidizes the AA leucine.

Table 3. Specific interaction between MAC and the AA leucine.

Nombre	Reducing agent	Oxidizing agent	HOMO	LUMO	Bg	δ–	δ+	EP	ETC
Ac. Málico	MAC	MAC	-11.410	0.548	11.958	-0.125	0.198	0.323	37.022
Leucina	Leu	Leu	-9.645	0.922	10.567	-0.126	0.13	0.256	41.279

Ac. Málico vs. Leucina	MAC	Leu	-11.410	0.922	12.332	-0.125	0.13	0.255	48.362
Leucina vs. Ac. Málico	Leu	MAC	-9.645	0.548	10.193	-0.126	0.198	0.324	31.460

The bottoms of the quantum wells are shown in Figure 3 (see Figure 1B). The red dot representing the Leu-MAC interaction falls in the high probability zone. For this reason, MAC will oxidize the AA Leu with a high probability. Instead, the blue dot falls in the zone of lowest probability; the AA Leu has a very low probability of oxidizing MAC.

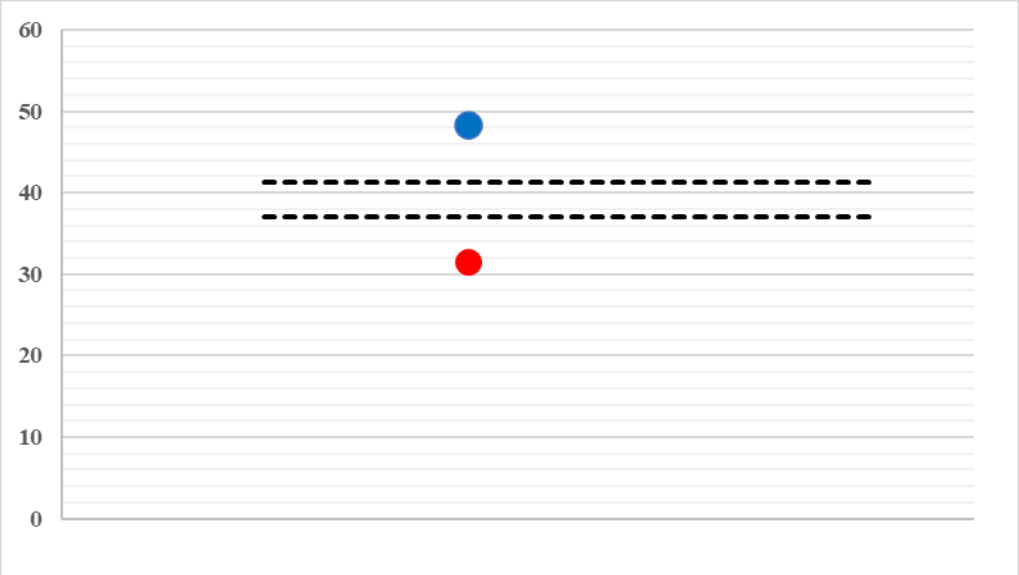

Figure 3. The red dot (Leu-MAC) is in a zone of high probability or affinity, and the blue dot (MAC-Leu) is in a low probability zone. In all interactions, Left = reducing agent, Right = oxidizing agent.

Table 4 shows us the specific interaction between MAC and the branched AA isoleucine. The first two lines show the two pure substances that interact. In row 3 we can see the MAC-Ile interaction with an ETC = 39.559 Bohr radii. In this interaction, isoleucine oxidizes MAC.
Row 4 shows the Ile-MAC interaction with an ETC = 31.963 Bohr radii. In this interaction, the MAC oxidizes the AA isoleucine.

Table 4. Specific interaction between MAC and the AA isoleucine.

Nombre	Reducing agent	Oxidizing agent	HOMO	LUMO	Bg	δ–	δ+	EP	ETC
Ac. Málico	MAC	MAC	-11.410	0.548	11.958	-0.125	0.198	0.323	37.022
Isoleucina	Ile	Ile	-9.872	0.972	10.844	-0.128	0.188	0.316	34.316
Ac. Málico vs. Isoleucina	MAC	Ile	-11.410	0.972	12.382	-0.125	0.188	0.313	39.559
Isoleucina vs. Ac. Málico	Ile	MAC	-9.872	0.548	10.420	-0.128	0.198	0.326	31.963

The bottoms of the quantum wells are shown in Figure 4 (see Figure 1B). The red dot representing the Ile-MAC interaction falls in the high probability zone. For this reason, MAC will oxidize the AA Leu with a high probability. Instead, the blue dot falls in the zone of lowest probability; the AA Ile has a very low probability of oxidizing MAC.

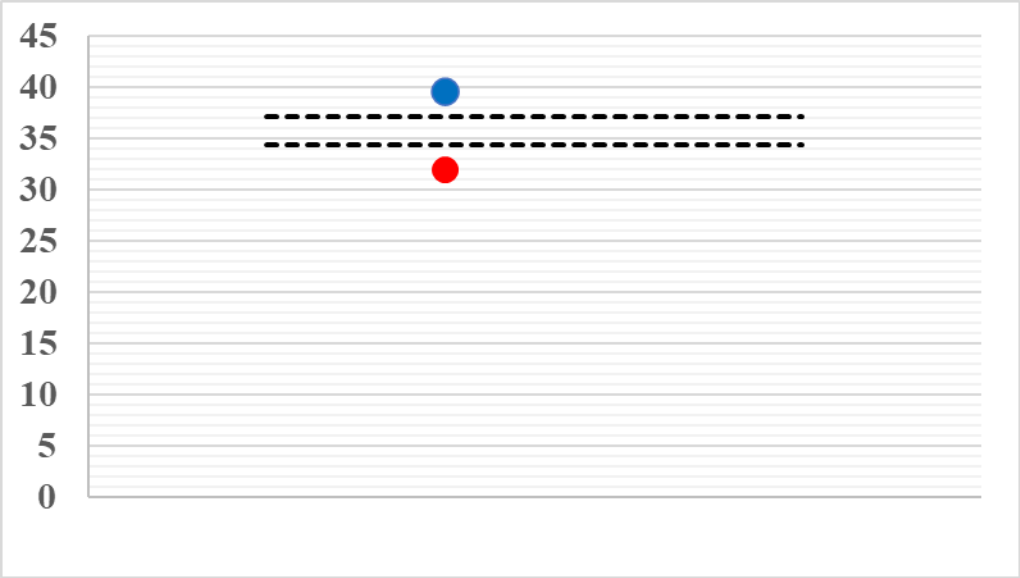

Figure 4. The red dot (Ile-MAC) is in a zone of high probability or affinity, and the blue (MAC-Ile) is in a low probability zone. Left = reducing agent, Right = oxidizing agent.

4. DISCUSSION

Yoo and Hand (2022), Ma et al. (2022), and Khan (2022) tell us that AAs help cancer cells (CC) counteract therapies. This help is due to maintaining CC redox homeostasis, biosynthetic processes, epigenetic modification, and metabolic intermediates for energy generation. Lin et al. (2022) mention that the ANGPTL4/BCAA/mTOR axis is an essential pathway in OS progression.
Other researchers mention the antioxidant and anticancer power of MAC. We found a probable and robust interaction between the three BCVAA AAs and MAC.

5. CONCLUSIONS

5.1 Hypothesis.

The three BCVAA AAs interact with a very high probability with MAC.

5.2 Thesis. We find that:

1. Interactions of BCVAAs and MAC are very likely and related.
2. In these three interactions, the oxidative character of MAC is shown.
A) The Val-MAC interaction with an ETC = 31.798 Bohr radii. In this interaction, the MAC oxidizes the AA valine.
B) The Leu-MAC interaction with an ETC = 31.460 Bohr radii. In this interaction, the MAC oxidizes the AA leucine.
C) The Ile-MAC interaction with an ETC = 31.963 Bohr radii. In this interaction, the MAC oxidizes the AA isoleucine.
3. The oxidative character has values very close to each other. This proximity of values indicates that they have a very similar affinity between the MAC and each of the BCVAA.
4. The chemical-quantum oxidation of AAs is an antioxidant for another type of interaction because the BCVAA molecule is already oxidized.

5.3 Corollary and arguments.
To reach these conclusions or theses, we.
1. We use the electron transfer coefficient theory.
2. We did a quantum-chemical analysis of the pure substances in Table 1.
3. We crossed ETC values to determine the quantum oxidation-reduction interactions.

4. We did a dichotomous analysis of each AA BCVAA with MAC.

REFERENCES

1. Yoo, H. C., & Han, J. M. (2022). Amino Acid Metabolism in Cancer Drug Resistance. Cells, 11(1), 140.
2. Ma, X., Ye, Y., Sun, J., Ji, J., Wang, J. S., & Sun, X. (2022). Coexposure of Cyclopiazonic Acid with Aflatoxin B1 Involved in Disrupting Amino Acid Metabolism and Redox Homeostasis Causing Synergistic Toxic Effects in Hepatocyte Spheroids. Journal of Agricultural and Food Chemistry.
3. Khan, S. U., & Khan, M. U. (2022). The Role of Amino Acid Metabolic Reprogramming in Tumor Development and Immunotherapy. Biochemistry and Molecular Biology, 7(1), 6-12.
4. Lin, S., Miao, Y., Zheng, X., Dong, Y., Yang, Q., Yang, Q., ... & Yuan, T. (2022). ANGPTL4 negatively regulates the progression of osteosarcoma by remodeling branched-chain amino acid metabolism. Cell death discovery, 8(1), 1-11.
5. Das, P. R., Darwish, A. G., Ismail, A., Haikal, A. M., Gajjar, P., Balasubramani, S. P., ... & El-Sharkawy, I. (2022). Diversity in blueberry genotypes and developmental stages enables discrepancy in the bioactive compounds, metabolites, and cytotoxicity. Food chemistry, 374, 131632.
6. Ersoy, E., Karahan, S., Boga, M., Cinar, E., Izgi, S., Mataraci Kara, E. … Eroğlu Özkan, E. (2022). Evaluation of the medicinal potential of a traditionally important plant from Turkey: Cerinthe minor L. İstanbul Journal of Pharmacy, 52(1), 80-89. DOI: 10.26650/IstanbulJPharm.2022.1001685.
7. Potapenko, Andrei A., "Characterization of L-malic acid-capped CdS Quantum Dots and Examination of the Nanoncrystal's Biosensor Ability" (2022). Honors Theses and Capstones. 620. https://scholars.unh.edu/honors/620
8. González-Pérez, M., Villafuerte-Salcedo, R. A., Briteño-Vázquez, M., González-Martínez, E. L., Gonzalez-Martinez, D., & Villafuerte-Díaz, R. (2020). Chemical-quantum analysis of the interactions of remdesivir vs. sars-cov-2 (covid-19) proteins. morbidity and mortality, 1, 3.
9. González-Pérez, M, Barroeta-Gómez, D., David Pérez-Sánchez, A., Suleni Rodríguez-Asenjo, Alondra (2022). World Journal of Pharmaceutical Research, 11(2) 40-47.
10. González-Pérez, M., Isasmendi-Cortés, M., Buendía-Córdova, J. S., Caamal-Mota, A., Castro-Jara, H., Zúñiga-Márquez, E. A., & de Román-Mello, V. H. (2021). Study of chemical-quantum interactions of structural amino acids of her-2 and quercetin. World Journal of Pharmaceutical Research. 10(14), 169-179.
11. González-Pérez, M., Hernández-Pérez, ML., Martínez-Velasco, A., Martínez-Castillo, G., Trejo-Mirón, JL, Hernández-Ortiz, A. (2021). World Journal of Pharmaceutical Research, 10(4), 1580-1592.
12. González-Pérez, M., & Sánchez-Parada, Oscar (2018). Demonstration of molecular oxidation throughquantum chemistry. World Journal of Pharmancy and Pharmaceutical Siencies (2018), 7(6), 1461-1469.